

# Digital Image Correlation Analysis of CFRP during compression test

C.Barile, C.Casavola, T.Mizzi, G.Pappalettera, C.Pappalettere

Politecnico di Bari,

Dipartimento di Meccanica, Matematica e Management, viale Japigia 182 -70126 Bari

## Abstract

The present paper examines the mechanical behavior of composite laminate subjected to uniaxial compression by DIC (Digital Image Correlation) 3D technique, in particular by analyzing the stability of the buckling equilibrium.

The purpose is how to measure the off-plane displacements, typically founded in buckling, in any point of the ROI (region of interest) of the investigated structure, using a full-field and non-contact measurement technique.

The innovative aspect of this work is therefore to solve this problem through an experimental approach with DIC 3D technique.

## 1 Introduction

Structures in composite materials are obtained by joining at least two materials, with very different physical and mechanical characteristics. The purpose of this matching is to obtain a final material with better characteristics than those referable to the single initial materials. The composite is generally made up by reinforcement and matrix, giving rise to a solid and continuous material, able to transmit and redistribute internal stress. We can state that composites are non-homogeneous and non-isotropic materials, where the individual constituents are bonded to each other in an insoluble way in order to obtain a final product that combines the best properties of the components. The Fiber Reinforced Polymers (FRP) analyzed in this work are made up by a carbon fiber material (reinforcement) and by epoxy resin as a matrix.

The main carbon fiber properties [1] are: high mechanical strength, high elastic modulus, low density, low crack sensitivity, fatigue resistance and good ability to dampen vibrations. Moreover, the thermal expansion coefficients allow having structures with dimensional stability over a great range of temperature variation.

Epoxy resins [2] represent a group of thermosetting polymeric materials that do not create reaction products when they cure (reticulate) and therefore have a low reticulation retention. They also have good adhesion to other materials, good chemical and environmental resistance, good mechanical properties and good electrical insulation properties. All of these features, together with a remarkable weight reduction combined with high strength (high SWR: strength to weight ratio), make possibility of combining those two materials very appealing in the aeronautic field.

Composites are non-homogeneous and anisotropic materials, so they respond differently to a given load, depending on the direction considered; as a consequence, a proper approach to material

characterization, should employ full-field measurement techniques as, for example, those based on Digital Image Correlation [3].

The three-dimensional DIC technique uses two cameras in order to look at the object from two different directions, obtaining a binocular view that allows to determine the three displacement coordinates (X, Y, Z) for each generic point of the analyzed area [4]. Measurement requires the application of a speckle random pattern on the specimen test.

The 3D DIC technique can also be applied to non-flat surfaces that are displaced off the plane, as in the case of buckling structures; in fact, it provides information about both the shape of the body and the three-dimensional strain field. For this purpose, several images are captured by the two cameras and the speckle pattern for each deformed configuration is analyzed with respect to a reference one.

## 2 Materials and Methods

### 2.1 Material description and preparation of the component for measurement

The material analyzed is a composite laminate made up of an epoxy resin mat with carbon fiber reinforcement.

The size of the component subjected to uniaxial compression is 150x100x5 (mm). The layout of the plies, according to the manufacturer's reference is as follows.

Type I layup: FF = 0T / 0F / 0T / 0T / 0F / 0T / 0T / 45F / 0T / SF where F = Fabric, T = Tape

The speckle pattern to be analyzed by DIC was introduced by spraying the specimen (Fig.1). To this scope a matt white spray and a black matt spray were used.

Four electrical strain gauges, two for each side of the pieces, were applied on each specimen [5], in order to evaluate the local strain

resulting from the application of compressive loads. in such a way it is possible to compare local behaviour obtainable by strain gages with overall behaviour obtained by DIC.

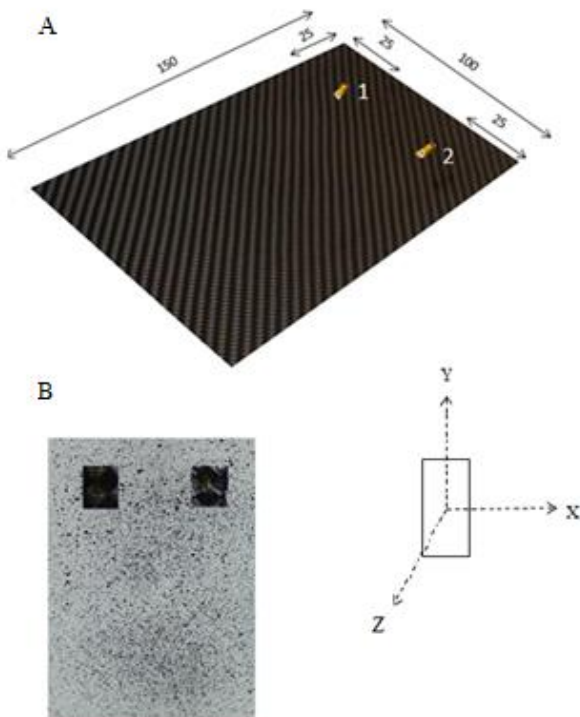


Figure 1. Composite laminate  
a) Extensimeter application allowances  
b) component prepared with speckle pattern

The strain gauges used are HBM LY1, with a measuring base  $l_0 = 3\text{mm}$ , gage factor  $k = 1.99$ .

The strain gauges adopted are able to evaluate deformations in one direction (uniaxial). Strain gages with a resistance of  $350\ \Omega$  were used because the composites are bad conductors.

## 2.2 Description of the compression test machine

Compression test were performed by following the ASTM 7137 (Compression After Impact "CAI") standard defined for the composite. In particular this standard specifies the applied constrains and the ambient condition and the compression rate.

Test were performed on a SCHENCK servo-hydraulic machine. In this machine the lower clamp is movable while the upper crosshead is fixed and must be initially positioned with the highest precision in order to avoid torsional or flexural deformations that could introduce errors in the measurement process. The main setting for the test are listed as below:

- Static test, then monotonic test
- Load cell from 250 KN

- Axial channel (being uniaxial compression)
- Control in "displacement rate" ( $1.25\ \text{mm} / \text{min}$  until breakage [5])
- Acquisition frequency of 10 HZ

## 2.3 Configuration of the measurement chain

For a greater accuracy of the tests and to measure the variables involved in the phenomenon of instability of the specimens, a measurement chain was required to complete the reading of displacements and deformations in a suitable manner.

In order to measure displacements and deformations of the whole surface of the specimens in the field three - dimensional, the Dynamics Q400 system with ISTR4 4D software was used.

It includes two Manta industrial cameras, with Ricoh 16mm lenses, fixed on the same support in order to avoid vibrations. System also includes a 4-channel data acquisition and synchronization unit and a light source.

Lighting is used to ensure that the speckle pattern on the specimen, once acquired, has a fairly wide grayscale span range; this means that the background is sufficiently clear (white) and dark (dark) without going into saturation in areas under DIC analysis , but also ensuring uniformity of luminance in these same areas.

It has been chosen to use an optic with a reduced focal length because the latter allow the capture of sufficiently large test specimens to monitor the whole component.

The cameras were coupled to a National Instruments® NIDAQ 9171 acquisition card which allows analog to digital conversion of the acquired signal.

To synchronize acquisition with the start of the test, a trigger signal exiting from the loading machine was sent to the acquisition system by a BNC cable.

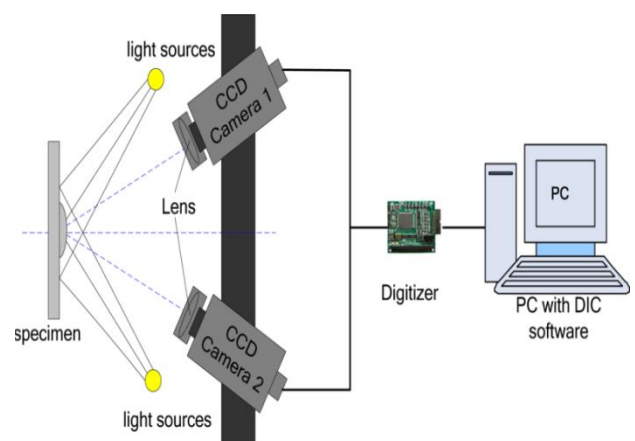


Figure 2. Schematic of a complete 3-D DIC system [6]

Settings for the DIC system are listed below:

- Distance between cameras  $l=40\text{cm}$
- Distance between lens and piece  $d=50\text{cm}$
- Inclination angle of the cameras  $=21.8^\circ$
- Diaphragm opening  $=f/8$



Figure 3. Overview of experimental set-up

The adopted compressive test fixture is shown in Figure 4.

It utilizes adjustable retention plates to support the specimen edges and inhibit buckling when the specimen is loaded.

The fixture consists of one base plate, two base slide plates, two angles, four side plates, one top plate, and two top slide plates. The side supports are knife edges, which provide no restraint to local out-of-plane rotation.

The top and bottom supports provide no clamp-up, but provide some rotational restraint due to the fixture geometry (the slide plates have a squared geometry and overlap the specimen by 8 mm [0.30 in.]). The fixture is adjustable to accommodate small variations in specimen length, width and thickness. The top plate and slide plates, which are not directly attached to the lower portion of the fixture, slip over the top edge of the test specimen. The side plates are sufficiently short to ensure that a gap between the side rails and the top plate is maintained during the test.

The configuration of the panel edge-constraint structure can have a significant effect on test results. In the standard test fixture, the top and bottom supports provide no clamp-up, but provide some restraint to local out-of-plane rotation due to the fixture geometry. The side supports are knife edges, which provide no rotational restraint.

Edge supports must be co-planar. Results are affected by the geometry of the various slide plates local to the specimen.

Results are also affected by the presence of gaps between the slide plates and the specimen, which can reduce the effective edge support and can result in concentrated load introduction conditions at the top and bottom specimen surfaces.

Additionally, results may be affected by variations in torque applied to the slide plate fasteners; loose fasteners may also reduce the effective edge support.



Figure 4. Edge-constraint structure adopted in the experiment

### 3 Results and Discussion

In order to measure the displacements and deformations of the entire surface of the composite in the three-dimensional field, the mechanical uniaxial compression test was monitored using the 3D system, acquiring a series of images that represent the displacement off the plane (z-displacement), starting from the first non-deformed configuration of the component until it came to break, with acquisition frequency of 1Hz, for the entire duration of the test.

The analysis of these frames (Fig.5), at certain steps, allows to view the buckling in CFRP subjected to uniaxial compression.

The images are captured and correlated by setting a "high accuracy" mode that allows a correlation with a 3d residuum of less than 0.4 pix, a facet size of 19 pixels and an accuracy of 0.1 pixels that allows locating 1180 grid point in the region of interest (ROI) of composite laminate.

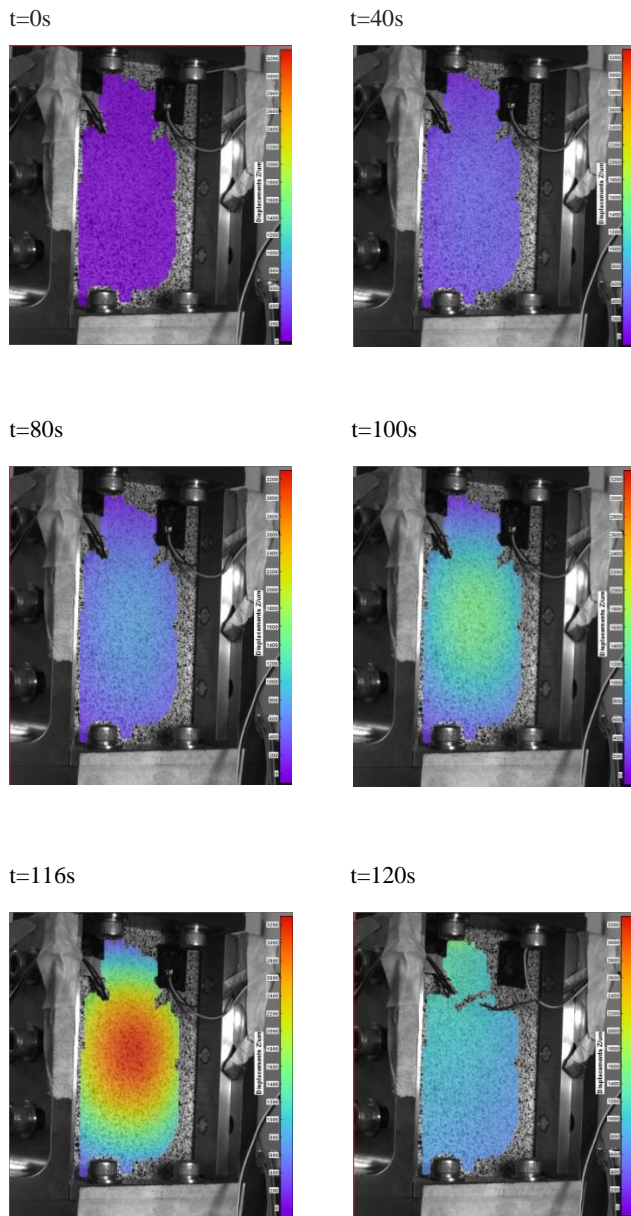


Figure 5. Frames of out of plane displacement of the composite taken by DIC at various steps

From the analysis of the images, the following considerations can be done: the component, due to the adopted fixtured and the low displacement rate implemented (1.25 mm / min) is subjected, in the first load steps to low out of plane displacement values (e.g. 400 μm at the center of the specimen at step t = 40s).

The component begins to buckle after 80 seconds from the beginning of the test when an out of plane displacement equal to 800 μm is recorded. After 116 s out of plane displacement becomes more evident and it reaches a value of 3200 μm while the specimen broke soon after, namely at 120 seconds.

Temporal load law is reported in Fig.6.

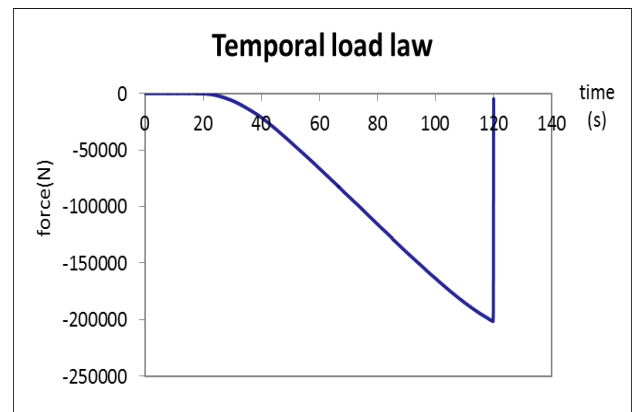
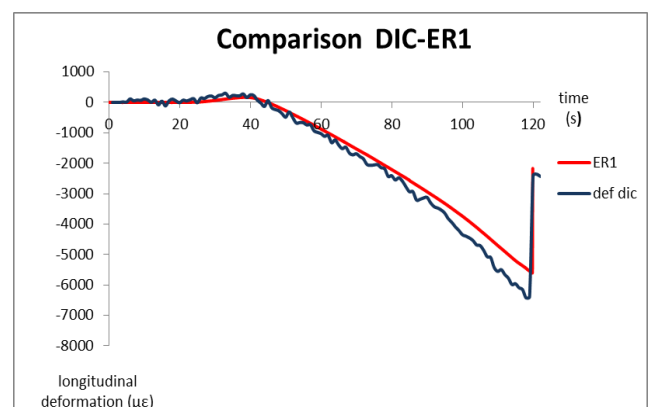


Figure 6. Temporal load law of the machine

There is a first hyperbolic trend in the first 40 s until reaching a load of about -21kN. At this point the first instability of the component is recorded because some out of plane displacement are observable at this point. Successively there is a linear behavior, which terminated at t= 80 seconds. From that point until 116 seconds a slight slope change occurs as a result of the buckling of the specimen as it is inferable by observing DIC images.

The abrupt cut of curve is caused by the breaking of the specimen with the consequent detachment of the supporting LVDTs immediately after reaching maximum load, recorded at the break of the sample at t = 120 s corresponding to F = -200 kN.

Using two additional electrical strain gauges at known locations [5] it has been possible a comparison between the  $\epsilon_{yy}$ -t results obtained by ER and DIC; to verify the accuracy the deformation  $\epsilon_{yy}$  value was read across the strain gauges 1 and 2 and it was compared to the corresponding DIC reading along a gauge of 3 mm corresponding to the measurement base  $l_0$  of the strain gauges, located at the points where ER were applied (Fig.7)



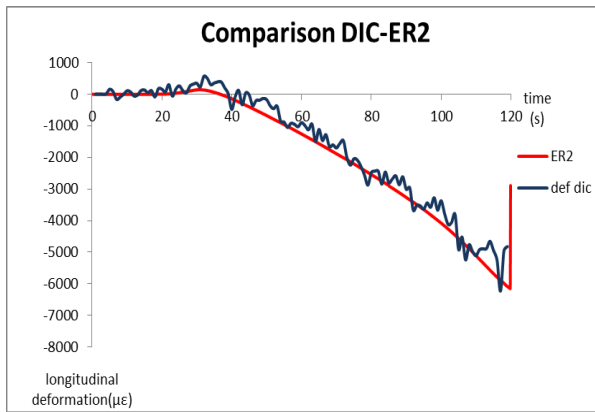


Figure 7. Comparison of longitudinal deformation reading between DIC and strain gauge

From the comparison between the two techniques it is possible to infer that there is some overlap in the deformation trends. For one of the two considered ER lower deformation where recorded; this may be due to a misalignment error in the mounting of the two strain gauges, in fact there is a certain shift between the left and right of the specimen with respect to the center of the latter in favor of the left area.

It should also be observed that higher level of noise affects the data obtained by DIC as reported in Fig.7 and this is due to the high luminance reflected by the bounding structure, on the right side where the ER2 is mounted.

In this case a "smoothing" operation is preferable.

In Fig.8 the trend of longitudinal deformation along the cross section of the specimen is shown, at the step  $t = 116s$ .

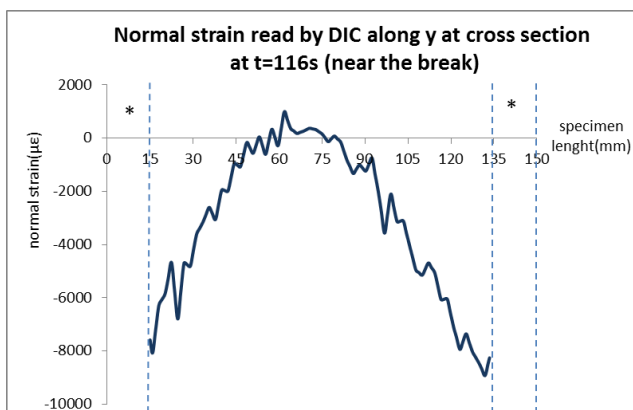


Figure 8. Normal strain  $\epsilon_{yy}$  at  $t=116s$

It can be noticed that the component has a normal strain  $\epsilon_{yy}$  negative in the outer areas, according to a nearly symmetrical pattern with respect to the center of the specimen. At the center the deformations are positive then the specimen stretches slightly.

There is a certain shift towards the top, in fact it is precisely in that area, exactly 15 mm from the 0 that breaks. In Fig 9 the shear strain recorded after 116 s is reported

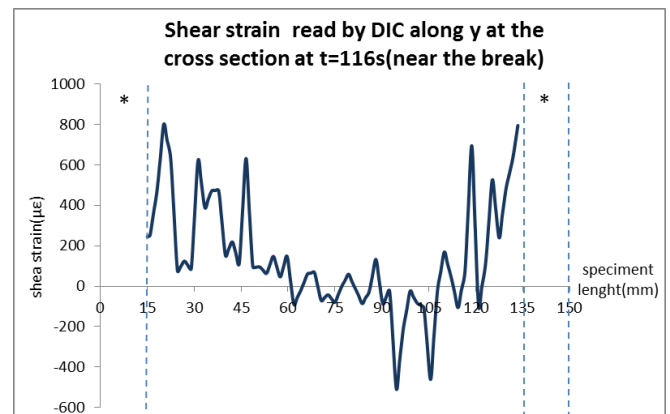


Figure 9. Shear strain  $\gamma_{xy}$  at  $t=116s$

Interesting considerations can be made on the previous graph.

It was noted that the maximum shear strain value can be traced from 15 to 20 mm from the zero and that is the point where the sample starts to break.

This may be understood in the framework of the continuum mechanics theory. Such deformation, in fact, is due to the sum of the mixed derivatives of the  $x$  e  $y$  displacements in response to the angular deformation of the composite in that area that determines delamination effects.

Previously indicated asymmetry was also found by analyzing the out of plane  $z$  displacements (Figure 10), in fact despite of the trend being typical of a gaussian, the lower part has a different slope than the upper one.

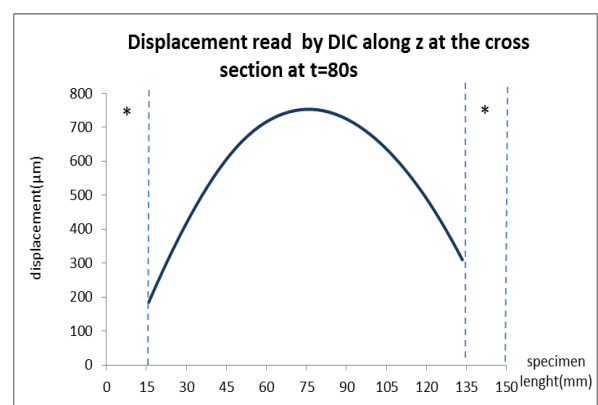


Figure 10. Out of plane displacement  $w$  at  $t=80s$

The off-plane displacement behaviour indicates how the specimen goes in buckling exactly at the center with a value of  $w = 750 \mu m$  at  $\frac{l}{2} = 75mm$ .

It can be stated, however, that although the specimen was constrained to a structure designed to avoid buckling, the

phenomenon of elastic instability is, however, at a critical load which is certainly higher than that referenced by the bibliography for a simply anisotropic supported plate subject to uniaxial compression [7].

The areas indicated by \* do not display information since in those areas the DIC was unable to recognize the speckle pattern and therefore could not read the u,v,w displacements along x, y, z.. The underlying reason for this lack of information is that the particular constrained structure creates shadow zone that do not allow the lenses to recognize the white and black points typical of the speckle pattern.

#### 4 Conclusions

In this paper the mechanical behavior of composite subjected to compression loading was reported as analyzed by Digital Image Correlation.

Electrical strain gauges at known locations [5] were also used in order to compare local results obtained by ER and full-field results obtained by DIC. This comparison underlines the possibility to apply the 3D DIC technique as an integration or a replacement of traditional measuring instruments to calculate displacements and deformations on the whole surface of the specimen. Allowing also reduction of some experimental bias as those connected with ER misalignment. Moreover, DIC is able to capture asymmetries in the behaviour of the sample, and this is a fundamental aspect for materials that are non-homogeneous and anisotropic.

#### Acknowledgment

Research co-funded by *Fondo di Sviluppo e Coesione 2007-2013 – APQ Ricerca Regione Puglia* “Regional program to support smart specialization and social and environmental sustainability – FutureinResearch”

#### References

- [1] F.C. Campbell Jr - *Manufacturing Technology for Aerospace Structural Materials*
- [2] I.K.Varma, V.B.Gupta, - *Thermosetting Resin Properties, Volume 2*; (ISBN: 0-080437206); IIT, Delhi, India.
- [3]Sutton, M.A., J.J. Orteu, and H.W. Schreier - *Image Correlation for Shape, Motion and Deformation Measurements*. Springer Science, 2009.
- [4]Ajovalasit, A. - *Analisi sperimentale delle tensioni con la fotomeccanica*, 2009
- [5] ASTM standard 7137 (Compression After Impact "CAI")

- [6] Yong-Kai Zhu <sup>1</sup>, Gui-Yun Tian <sup>1,2,\*</sup>, Rong-Sheng Lu <sup>3</sup> and Hong Zhang <sup>2</sup> - *A Review of Optical NDT Technologies*
- [7]. N. S. Trahair - *Flexural torsional buckling of structures*, CRC Press, 1993